Fully Distributed Analysis of MOS Transistor at Millimeter-Wave Band, Based on Matrix-Functions of the Three Line Active Transmission Lines Model

H. Khoshniyat, A. Abdipour, and G. Moradi

Department of Electrical Engineering, Institute of Communications Technology and Applied Electromagnetics
Amirkabir University of Technology, Tehran, 15914, Iran
hkhoshniyat@aut.ac.ir, abdipour@aut.ac.ir, ghmoradi@aut.ac.ir

Abstract ─ In this paper, distributed model of MOS transistor is presented that is based on active multi-conductor transmission line model. The analysis is done in frequency domain by considering frequency dependence of primary parameters such as series resistance caused by skin effect. The analysis is performed based on matrix function that is calculated by eigenvalue approach in the frequency domain. The scattering parameters are computed by using transmission matrix and applying boundary conditions. To investigate the analysis, the scattering parameters of a 0.13 μm transistor are calculated by proposed approach over the 1–100 GHz frequency band. They compared with the results obtained from the available lumped and distributed models and a commercial simulator that have a good agreement with each other.

Index Terms ─ Active multi transmission lines, distributed analysis, matrix function, MOS transistor, skin effect.

I. INTRODUCTION

Nowadays, the demand for low cost implementation of monolithic microwave integrated circuits leads to considerable progress in CMOS technology [1, 2]. Modern CMOS technologies have been matured enough for using in mm-wave applications. An accurate modeling of high frequency effect in millimeter wave is required for successful design of integrated CMOS circuits [3, 4]. By increasing the operating frequency of MOSFET to mm-wave band, the width of transistor becomes comparable to the wavelength. In such cases, the wave propagation through transistor's electrodes and distributed transmission line effects need to be studied accurately, in device modeling.

In [5], [6] and [7] the distributed transmission line effect along the gate width has been investigated. In these models, the gate electrode is divided into finite number of segments that are connected together by using of series of scaled gate resistor. In [8], the distributed transmission line signal and noise modeling of millimeter wave CMOS transistor is studied. The MOSFET transistor is considered as coupled active transmission lines structure, exciting by the noise equivalent sources distributed on its conductors.

In [9], distributed modeling of field effect transistors in the case of GaAs MESFET is studied. The transistor is considered as a multi-conductor active transmission line and the equations are solved by the Finite-Difference Time-Domain (FDTD) technique. According to this approach, the fully distributed analysis of CMOS transistor in the time domain has been studied in [10], based on the active multi-conductor transmission lines model.

In this paper, distributed model of MOS transistor based on active multi-conductor transmission line is presented. The analysis is performed in the frequency domain by considering frequency dependence of primary parameters such as series resistance that caused by skin effect. Based on matrix function calculated by eigenvalue approach, the analysis is done in the frequency domain. The scattering parameters are computed by using transmission matrix and applying boundary conditions. To verify the analysis, the scattering parameters of a 0.13 μm transistor are calculated by proposed approach over the 1–100 GHz frequency band and compared with the results obtained from the available lumped and distributed models and Cadence SpectreRF simulator that shown a good agreement with each other.

II. DISTRIBUTED MODEL OF TRANSISTOR

The schematic of MOSFET, is shown in Fig. 1. At high frequencies, the wavelength becomes comparable to the width of transistor and wave propagation through transistor's electrodes must be assumed. To consider this distributed effect, MOSFET can be modeled as three coupled transmission lines.

Submitted On: May 30, 2016
Accepted On: September 9, 2016

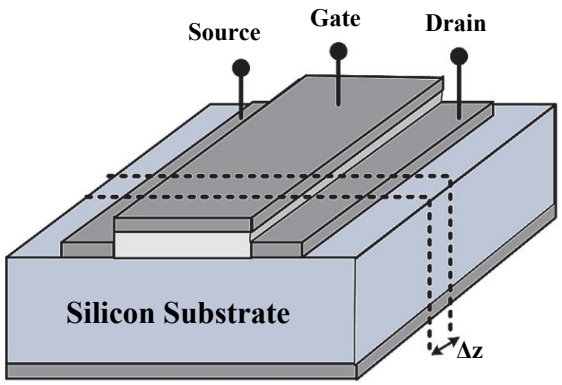

Fig. 1. The schematic of MOSFET as three coupled transmission lines on silicon substrate.

A. Transmission line model and equations

By considering the differential width of Δz (Δz << $\lambda_g(f_{max})$), the partial equivalent model of MOSFET is obtained as shown in Fig. 2. The equivalent model of MOSFET is combination of active and passive parts. Active part explains the behavior of intrinsic device while the passive part shows electromagnetic interaction between electrodes.

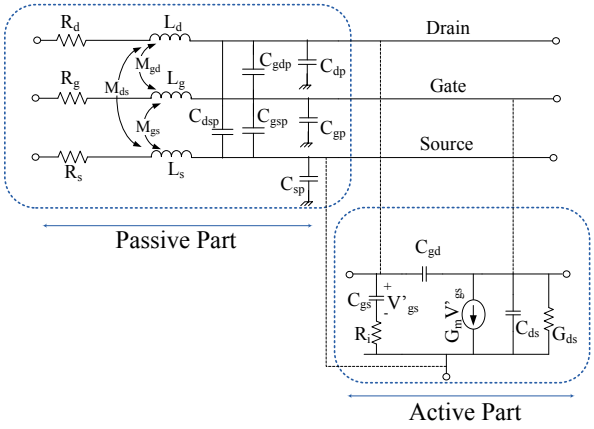

Fig. 2. The equivalent model of MOSFET.

By using of Kirchhoff's circuit laws, the matrix equations are achieved in the phasor domain as [11]:

$$\frac{d\mathbf{V}(z,\omega)}{dz} = -\mathbf{Z}_s(\omega)\mathbf{I}(z,\omega), \tag{1}$$

$$\frac{d\mathbf{I}(z,\omega)}{dz} = -\mathbf{Y}_p(\omega)\mathbf{V}(z,\omega). \tag{2}$$

The voltage and current matrices are defined as:

$$\mathbf{V}(z,\omega) = \begin{bmatrix} V_d & V_g & V_s \end{bmatrix}^T (z,\omega), \tag{3}$$

$$\mathbf{I}(z,\omega) = \begin{bmatrix} I_d & I_g & I_s \end{bmatrix}^T (z,\omega). \tag{4}$$

The series impedance and parallel admittance matrices are defined as:

$$\mathbf{Z}_s = \mathbf{R} + j\omega\mathbf{L}, \tag{5}$$

$$\mathbf{Y}_p = \mathbf{Y}_{TL} + \mathbf{Y}_{FET} = j\omega\mathbf{C} + \mathbf{Y}_{FET}. \tag{6}$$

Based on equivalent model, the primary matrices $(\mathbf{R},\mathbf{L},\mathbf{C})$ and $\mathbf{Y}_{FET}$ are obtained as shown in equations (7-10):

$$\mathbf{R} = \begin{bmatrix} R_d & 0 & 0 \\ 0 & R_g & 0 \\ 0 & 0 & R_s \end{bmatrix}, \tag{7}$$

$$\mathbf{L} = \begin{bmatrix} L_d & M_{gd} & M_{ds} \\ M_{gd} & L_g & M_{gs} \\ M_{ds} & M_{gs} & L_s \end{bmatrix}, \tag{8}$$

$$\mathbf{C} = \begin{bmatrix} C_{dp}+C_{gdp}+C_{dsp} & -C_{gdp} & -C_{dsp} \\ -C_{gdp} & C_{gp}+C_{gdp}+C_{gsp} & -C_{gsp} \\ -C_{dsp} & -C_{gsp} & C_{sp}+C_{dsp}+C_{gsp} \end{bmatrix}, \tag{9}$$

$$\mathbf{Y}_{FET} = \begin{bmatrix} Y_{11} & Y_{12} & Y_{13} \\ Y_{21} & Y_{22} & Y_{23} \\ Y_{31} & Y_{32} & Y_{33} \end{bmatrix},$$

$$Y_{11} = G_{ds} + j\omega(C_{gd}+C_{ds}), Y_{12} = -j\omega C_{gd} + G_m \frac{1}{1+j\omega R_i C_{gs}},$$

$$Y_{13} = -G_{ds} - j\omega C_{ds} - G_m \frac{1}{1+j\omega R_i C_{gs}}, Y_{21} = -j\omega C_{gd},$$

$$Y_{22} = j\omega C_{gd} + \frac{j\omega C_{gs}}{1+j\omega R_i C_{gs}}, Y_{23} = -\frac{j\omega C_{gs}}{1+j\omega R_i C_{gs}},$$

$$Y_{31} = -G_{ds} - j\omega C_{ds}, Y_{32} = -\frac{G_m + j\omega C_{gs}}{1+j\omega R_i C_{gs}},$$

$$Y_{33} = \frac{G_m + j\omega C_{gs}}{1+j\omega R_i C_{gs}} + G_{ds} + j\omega C_{ds}. \tag{10}$$

By considering the skin effect, the series resistance is proportional to the square of frequency and can be represented as:

$$R_i = \chi_i \sqrt{f} \qquad i = g,d,s\ . \tag{11}$$

In Fig. 3, the schematic of simulated MOSFET is shown. Based on chain matrix, the $\mathbf{V}$ and $\mathbf{I}$ matrices at $z=0$ are calculated from the $\mathbf{V}$ and $\mathbf{I}$ matrices at $z=l$. This is expressed with matrix-functions as [11]:

$$\begin{bmatrix} \mathbf{V}(0) \\ \mathbf{I}(0) \end{bmatrix} = \begin{bmatrix} \cosh(\sqrt{\mathbf{Z}_s\mathbf{Y}_p}\,l) & \sinh(\sqrt{\mathbf{Z}_s\mathbf{Y}_p}\,l)\mathbf{Z}_C \\ \mathbf{Z}_C^{-1}\sinh(\sqrt{\mathbf{Z}_s\mathbf{Y}_p}\,l) & \mathbf{Y}_p\cosh(\sqrt{\mathbf{Z}_s\mathbf{Y}_p}\,l)\mathbf{Y}_p^{-1} \end{bmatrix} \begin{bmatrix} \mathbf{V}(l) \\ \mathbf{I}(l) \end{bmatrix}. \tag{12}$$

The characteristic impedance matrix ($\mathbf{Z}_C$) can be written as [11]:

$$\mathbf{Z}_C = \mathbf{Y}_P^{-1}\sqrt{\mathbf{Y}_P\mathbf{Z}_s} = \mathbf{Z}_s\left(\sqrt{\mathbf{Y}_P\mathbf{Z}_s}\right)^{-1}. \tag{13}$$

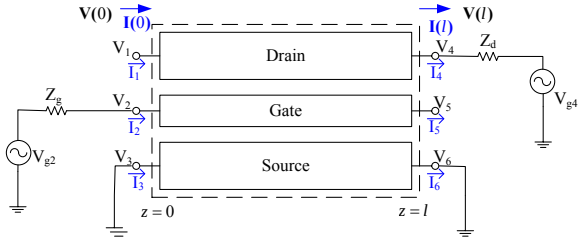

Fig. 3. The schematic of simulated MOSFET.

B. Intrinsic parameters of MOSFET

The intrinsic parameters of MOS transistor including G_m, C_{gs}, C_{ds}, C_{gd}, R_i, and G_{ds} (active part parameters) are calculated based on the accurate physical model of the MOSFET, BSIM3v3. The drain-source current by using a complete single equation for both linear and saturation regions is expressed as:

$$I_{ds} = \frac{I_{ds0}(V_{dseff})}{1+\dfrac{R_{ds}I_{ds0}(V_{dseff})}{V_{dseff}}}\left(1+\frac{V_{ds}-V_{dseff}}{V_A}\right) \cdot \left(1+\frac{V_{ds}-V_{dseff}}{V_{ASCBE}}\right). \tag{14}$$

The transistor conductance G_m can be obtained as:

$$G_m = \left.\frac{\partial I_{ds}}{\partial V_{gs}}\right|_{V_{ds=Const.}}. \tag{15}$$

Also, all capacitances are derived from the charges to ensure charge conservation as:

$$C_{ij} = \frac{\partial Q_i}{\partial V_j};\ \ i,j = g,d,s,b\ \ , \tag{16}$$

where the terminal charges Q_g, Q_b, Q_s, and Q_s are the charges associated with the gate, bulk, source, and drain terminals, respectively. The details of this model containing other equations and the parameters description are given in [12].

C. Solving equations

As shown in Fig. 3, the chain matrix can be assumed as a six-port network that ports 1, 2 and 3 are inputs ($z=0$) and ports 4, 5 and 6 are outputs ($z=l$). The six-port matrix ($\mathbf{T}$) equation is shown as:

$$\begin{bmatrix} V_1 \\ V_2 \\ V_3 \\ I_1 \\ I_2 \\ I_3 \end{bmatrix} = \begin{bmatrix} T_{11} & T_{12} & T_{13} & T_{14} & T_{15} & T_{16} \\ T_{21} & T_{22} & T_{23} & T_{24} & T_{25} & T_{26} \\ T_{31} & T_{32} & T_{33} & T_{34} & T_{35} & T_{36} \\ T_{41} & T_{42} & T_{43} & T_{44} & T_{45} & T_{46} \\ T_{51} & T_{52} & T_{53} & T_{54} & T_{55} & T_{56} \\ T_{61} & T_{62} & T_{63} & T_{64} & T_{65} & T_{66} \end{bmatrix} \begin{bmatrix} V_4 \\ V_5 \\ V_6 \\ I_4 \\ I_5 \\ I_6 \end{bmatrix}. \tag{17}$$

Based on Fig. 3, the boundary conditions are applied to matrix equation that is shown as:

$$\begin{bmatrix} V_1 \\ V_2 \\ 0 \\ 0 \\ \dfrac{V_{g2}-V_2}{Z_g} \\ I_3 \end{bmatrix} = \begin{bmatrix} T_{11} & T_{12} & T_{13} & T_{14} & T_{15} & T_{16} \\ T_{21} & T_{22} & T_{23} & T_{24} & T_{25} & T_{26} \\ T_{31} & T_{32} & T_{33} & T_{34} & T_{35} & T_{36} \\ T_{41} & T_{42} & T_{43} & T_{44} & T_{45} & T_{46} \\ T_{51} & T_{52} & T_{53} & T_{54} & T_{55} & T_{56} \\ T_{61} & T_{62} & T_{63} & T_{64} & T_{65} & T_{66} \end{bmatrix} \begin{bmatrix} V_4 \\ V_5 \\ 0 \\ \dfrac{V_4-V_{g4}}{Z_d} \\ 0 \\ I_6 \end{bmatrix}. \tag{18}$$

In Equation (18), V_1, V_2, V_4, V_5, I_3 and I_6 are unknowns while the elements of $\mathbf{T}$ (T_{ij}), Z_g and Z_d are knowns; V_{g2} and V_{g4} are input voltages for calculating scattering parameters. The unknowns ($\mathbf{X}$) and input voltages ($\mathbf{V_g}$) are considered as:

$$\mathbf{X} = \begin{bmatrix} V_1 & V_2 & V_4 & V_5 & I_3 & I_6 \end{bmatrix}^T, \tag{19}$$

$$\mathbf{V_g} = \begin{bmatrix} 0 & V_{g2} & 0 & V_{g4} & 0 & 0 \end{bmatrix}^T. \tag{20}$$

By arranging Equation (18) based on unknowns ($\mathbf{X}$) and input voltages ($\mathbf{V_g}$), the matrix equation with coefficient matrices ($\mathbf{A}$ and $\mathbf{B}$) is obtained as:

$$\mathbf{AX} = \mathbf{BV_g}, \tag{21}$$

$$\mathbf{X} = \mathbf{A}^{-1}\mathbf{BV_g}. \tag{22}$$

For example, by sorting the first row of Equation (18), the first row of $\mathbf{A}$ and $\mathbf{B}$ are achieved as:

$$\begin{aligned} V_1 &= T_{11}V_4 + T_{12}V_5 + T_{14}\frac{V_4 - V_{g4}}{Z_d} + T_{16}I_6, \\ \frac{T_{14}}{Z_d}V_{g4} &= -V_1 + \left(T_{11} + \frac{T_{14}}{Z_d}\right)V_4 + T_{12}V_5 + T_{16}I_6. \end{aligned} \tag{23}$$

By arranging the other rows of Equation (18), the coefficient matrices ($\mathbf{A}$ and $\mathbf{B}$) are obtained as:

$$\mathbf{A} = \begin{bmatrix} -1 & 0 & T_{11}+\dfrac{T_{14}}{Z_d} & T_{12} & 0 & T_{16} \\ 0 & -1 & T_{21}+\dfrac{T_{24}}{Z_d} & T_{22} & 0 & T_{26} \\ 0 & 0 & T_{31}+\dfrac{T_{34}}{Z_d} & T_{32} & 0 & T_{36} \\ 0 & 0 & T_{41}+\dfrac{T_{44}}{Z_d} & T_{42} & 0 & T_{46} \\ 0 & \dfrac{1}{Z_g} & T_{51}+\dfrac{T_{54}}{Z_d} & T_{52} & 0 & T_{56} \\ 0 & 0 & T_{61}+\dfrac{T_{64}}{Z_d} & T_{62} & -1 & T_{66} \end{bmatrix}, \tag{24}$$

$$\mathbf{B}=\begin{bmatrix} 0 & 0 & 0 & \frac{T_{14}}{Z_d} & 0 & 0 \\ 0 & 0 & 0 & \frac{T_{24}}{Z_d} & 0 & 0 \\ 0 & 0 & 0 & \frac{T_{34}}{Z_d} & 0 & 0 \\ 0 & 0 & 0 & \frac{T_{44}}{Z_d} & 0 & 0 \\ 0 & \frac{1}{Z_g} & 0 & \frac{T_{54}}{Z_d} & 0 & 0 \\ 0 & 0 & 0 & \frac{T_{64}}{Z_d} & 0 & 0 \end{bmatrix}. \quad (25)$$

D. Computing scattering parameters

Based on scattering matrix definition, by assuming port 2 as input port and port 4 as output port, the scattering parameters are obtained as:

$$S_{11}, S_{21}\Big|_{V_{gi}=V_{g2}=V_g \;\&\; V_{go}=V_{g4}=0}, \quad (26)$$

$$\mathbf{V_g}=\begin{bmatrix}0 & V_g & 0 & 0 & 0 & 0\end{bmatrix}^T. \quad (27)$$

By considering $\mathbf{V_g}$ as was defined in (27), the unknown matrix ($\mathbf{X}$) is computed from (22) and input and output voltages are extracted as:

$$V_i=V_2=X(2)\ ,\ V_o=V_4=X(3). \quad (28)$$

The forward and backward voltage wave at input and output ports are defined as:

$$I_2=\frac{V_{g2}-V_2}{Z_g},$$

$$V_i^+=V_2^+=\frac{1}{2}\left(V_2+Z_gI_2\right)=\frac{V_{g2}}{2}, \quad (29)$$

$$V_i^-=V_2^-=\frac{1}{2}\left(V_2-Z_gI_2\right)=V_2-\frac{V_{g2}}{2},$$

$$I_4=\frac{V_4-V_{g4}}{Z_d},$$

$$V_o^+=V_4^+=\frac{1}{2}\left(V_4-Z_dI_4\right)=\frac{V_{g4}}{2}, \quad (30)$$

$$V_o^-=V_4^-=\frac{1}{2}\left(V_4+Z_dI_4\right)=V_4-\frac{V_{g4}}{2}.$$

The S_{11} and S_{21} are calculated as:

$$S_{11}=\frac{V_i^-}{V_i^+}\Big|_{V_{g4}=0}, \quad (31)$$

$$S_{21}=\frac{V_o^-}{V_i^+}\Big|_{V_{g4}=0}. \quad (32)$$

Similarly when $V_{gi}=V_{g2}=0$ and $V_{go}=V_{g4}=V_g$, the S_{12} and S_{22} are computed as:

$$S_{12}=\frac{V_i^-}{V_o^+}\Big|_{V_{g2}=0}, \quad (33)$$

$$S_{22}=\frac{V_o^-}{V_o^+}\Big|_{V_{g2}=0}. \quad (34)$$

The step by step procedure of fully distributed analysis in the frequency domain is shown in Fig. 4.

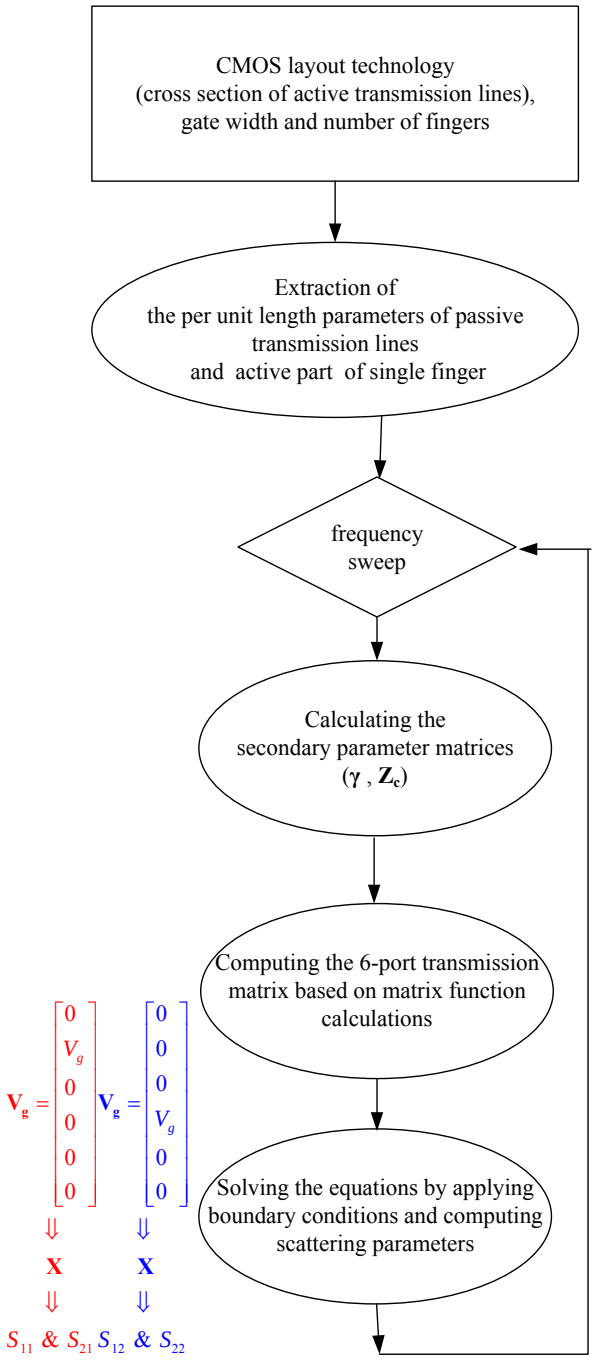

Fig. 4. The step by step flowchart of the proposed fully distributed method.

III. REULTS AND DISCUSSION

In order to analyze the MOS transistor with the proposed method, a single finger MOSFET with gate dimension of 0.13×10 μm is studied as shown in Fig. 3. In this example, both R_g and R_d are assumed to be 50 Ω. The end of gate electrode and the beginning of drain electrode are open, while both sides of the source electrode are grounded.

The per-unit-length parameters of the intrinsic MOSFET (active parameters) are achieved by using the BSIM3v3 model at the V_{gs}=1.2 V and V_{ds}=1.2 V bias point, with applying scaling technique. The per-unit-length capacitance and inductance matrixes of the passive part of the transistor are numerically specified by solving the two-dimensional electrostatic field problem in the cross section of each transmission lines. The per-unit-length resistances of the passive part of the MOSFET are obtained by considering the skin effect of the transistor electrodes. The achieved parameters are shown in Table 1 [10].

Table 1: The parameters of the passive part of distributed model [10]

Parameter	Value
L_d	1.919 μH/m
L_s	1.919 μH/m
L_g	1.95 μH/m
M_{gd}	1.54 μH/m
M_{gs}	1.54 μH/m
M_{ds}	1.407 μH/m
χ_d	3.2255 Ω. Hz $^{-0.5}$/m
χ_s	3.9781 Ω. Hz $^{-0.5}$/m
χ_g	3.2255 Ω. Hz $^{-0.5}$/m
C_{gp}	136.75 pF/m
C_{dp}	110.5 pF/m
C_{sp}	110.5 pF/m
C_{gdp}	63.07 pF/m
C_{gsp}	63.07 pF/m
C_{dsp}	29.65 pF/m

The scattering parameters of the transistor are obtained by the proposed approach at 1-100 GHz and compared with those of achieved by lumped model of the MOS transistor, distributed gate model [7], distributed time domain analysis [10] and also Cadence simulator. The scattering parameters are shown in Fig. 5. It seems that the results of all methods are in good agreement at low frequencies. But, the difference between the results becomes larger by increasing the frequency. Especially at higher frequencies, the results of proposed distributed approach are closer to the Cadence SpectreRF simulator results. At high frequencies the transistor width become order of the wavelength and this justified difference between various modeling approaches obviously. In such cases, the distributed analysis of the transistor based on multi conductor transmission lines can explain the behavior of the device at high frequencies more precise than others. Also, the frequency dependence of series resistance that caused by skin effect is considered by using the frequency domain approach based on transmission matrix equation.

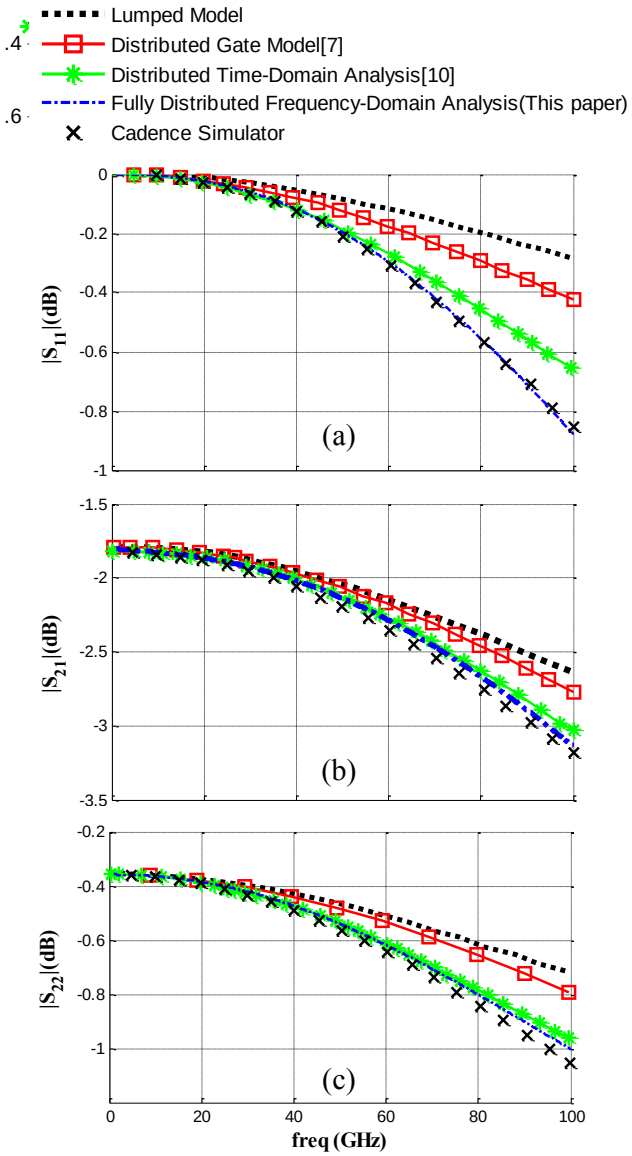

Fig. 5. The scattering parameters of the MOSFET: (a) S_{11}, (b) S_{21}, and (c) S_{22}.

The G_{MAX} versus frequency is one of the behavioral parameters of transistor that defined based on scattering parameters as [13]:

$$G_{MAX} = \begin{cases} MAG = (K - \sqrt{K^2 - 1}) \dfrac{|S_{21}|}{|S_{12}|} & K > 1 \\ \\ MSG = \dfrac{|S_{21}|}{|S_{12}|} & K < 1 \end{cases}, \quad (35)$$

where K (Rollet stability factor) is defined as:

$$K = \frac{1 - |S_{11}|^2 - |S_{22}|^2 + |\Delta|^2}{2|S_{21}S_{12}|}, \quad (36)$$

$$\Delta = S_{11}S_{22} - S_{12}S_{21}. \quad (37)$$

In Fig. 6, maximum gain versus frequency is shown for the 8-finger 0.13µm×50µm MOSFET. The behavior of transistor is analyzed with different methods (lumped model, semi distributed (5 and 50 slices) and fully distributed methods). Results of semi distributed model with the large number of sections have a good agreement with that of fully distributed model. Based on this graph, the f_{max} of transistor was extracted around 60 GHz.

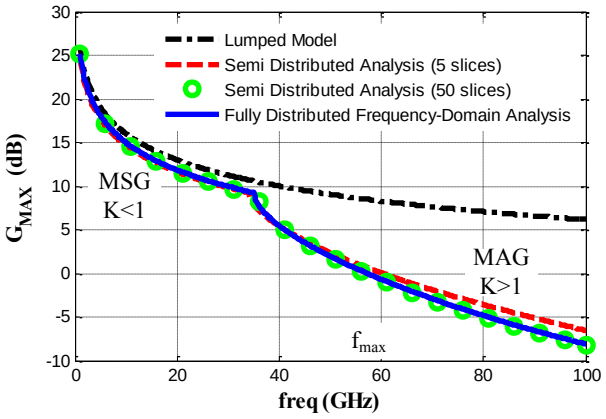

Fig. 6. Gmax (Maximum Available Gain (MAG) and Maximum Stable Gain (MSG)) versus frequency with lumped, semi and fully distributed analysis.

IV. CONCLUSION

The fully distributed analysis for high frequency MOSFETs based on three coupled transmission lines structure has been proposed. The matrix-based equations of that structure are extracted and solved using the frequency domain matrix function with applying boundary conditions and considering the frequency dependence of series resistance. By using the proposed method for a 0.13 µm MOS transistor, the small signal parameters have been obtained at 1–100 GHz and compared with the conventional models. Results of the proposed method present a good agreement with other models at low frequencies. But for the higher frequencies the differences become considerable and the calculated result of proposed approach is closer to the commercial simulator. Thus, the three-conductor transmission line modeling of MOS transistors in the frequency domain is more accurate than other conventional methods.

APPENDIX A. FUNCTIONS OF MATRICES

Computing a function $f(\mathbf{A})$ of an n-by-n matrix $\mathbf{A}$ is a popular problem in many application domains. If $\mathbf{A} \in \mathbb{C}^{n \times n}$ is diagonalizable, then it is particularly easy to specify $f(\mathbf{A})$ in terms of $\mathbf{A}$'s eigenvalues and eigenvectors [14].

If $\mathbf{A} \in \mathbb{C}^{n \times n}$, $\mathbf{A} = \mathbf{X}.diag(\lambda_1,...,\lambda_n).\mathbf{X}^{-1}$, and $f(\mathbf{A})$ is defined, then

$$f(\mathbf{A}) = \mathbf{X}.diag(f(\lambda_1),..., f(\lambda_n)).\mathbf{X}^{-1} \quad . \quad (A\text{-}1)$$

By using of matrix relations, the matrix function can be represented easily as:

$$f(\mathbf{A}) = \mathbf{X}.f(\mathbf{X}^{-1}.\mathbf{A}.\mathbf{X}).\mathbf{X}^{-1} \quad . \quad (A\text{-}2)$$

REFERENCES

[1] Z. Y. Cui, J. W. Park, C. S. Lee, and N. S. Kim, "Integration of CMOS logic circuits with lateral power MOSFET," *2013 4th International Conference on Intelligent Systems Modelling & Simulation (ISMS)*, pp. 615-618, Jan. 2013.

[2] A. M. Niknejad and H. Hashemi, *mm-Wave Silicon Technology 60 GHz and Beyond*. Springer Science+Business Media, LLC, 2008.

[3] S. Ma, J. Ren, and H. Yu, "An overview of new design techniques for high performance CMOS millimeter-wave circuits," in Proc. 14th Int. Symp. Integrated Circuits (ISIC), pp. 292-295, Dec. 2014.

[4] A. A. Abidi, "CMOS microwave and millimeter-wave ICs: The historical background," *in Proc. IEEE Int. Symp. Radio-Frequency Integrated Technology (RFIT)*, pp. 1-5, Aug. 2014.

[5] B. Razavi, R.-H. Yan, and K. F. Lee, "Impact of distributed gate resistance on the performance of MOS devices," *IEEE Trans. Circuits Syst. I*, vol. 41, pp. 750-754, Nov. 1994.

[6] E. Abou-Allam and T. Manku, "A small signal MOSFET model for radio frequency IC applications," *IEEE Trans. Computer-Aided Design*, vol. 16, pp. 437-447, May 1997.

[7] E. Abou-Allam and T. Manku, "An improved transmission-line model for MOS transistors," *IEEE Transaction on Circuits and Systems*, vol. 46, pp. 1380-1387, May 1999.

[8] Z. Seifi, A. Abdipour, and R. Mirzavand, "Distributed signal and noise modeling of millimeter wave transistor based on CMOS technology," *Applied Computational Electro-magnetics Society (ACES) Journal*, vol. 30, no. 8, pp. 915-921, Aug. 2015.

[9] K. Afrooz, A. Abdipour, A. Tavakoli, and Movahhedi, "FDTD analysis of small signal model for GaAs MESFETs based on three line structure,"

Asia-Pacific Microwave Conference APMC, pp. 1-4, 2007.
[10] F. Daneshmandian, A. Abdipour, and R. Mirzavand, "A three-conductor transmission line model for MOS transistors," *Applied Computational Electromagnetics Society (ACES) Journal*, vol. 30, no. 6, pp. 670-676, June 2015.
[11] C. R. Paul, *Analysis of Multiconductor Transmission Lines*. 2nd edition, John Wiley & Sons, Inc., Hoboken, New Jersey, 2008.
[12] C. Yuhua, et al., "*BSIM3v3 Manual: Final version*," University of California, Berkeley, 1996.
[13] J. Rollett, "Stability and power-gain invariants of linear two ports," *in IRE Transactions on Circuit Theory*, vol. 9, no. 1, pp. 29-32, Mar. 1962.
[14] G. H. Golub and C. F. Van Loan, *Matrix Computations*. 4th edition, The Johns Hopkins University Press, Baltimore, 2013.

Hamed Khoshniyat was born in Karaj, Iran, in 1985. He received the B.Sc. and M.Sc. degrees from the Amirkabir University of Technology (Tehran Polytechnic), Tehran, Iran, both in Electrical Engineering, in 2008 and 2010 respectively. He is currently working toward the Ph.D. degree in "Fields and Waves" and a Research Assistant in the Wave Propagation and Microwave Measurement Laboratory (WPMML) in Electrical Engineering at Amirkabir University of Technology (Tehran Polytechnic). His current research interests include analysis and modeling of distributed amplifiers and switches, non-Foster elements, active and passive microwave device and circuits and microwave measurement.

Abdolali Abdipour was born in Alashtar, Iran, in 1966. He received his B.Sc. degree in Electrical Engineering from Tehran University, Tehran, Iran, in 1989, his M.Sc. degree in Electronics from Limoges University, Limoges, France, in 1992, and his Ph.D. degree in Electronic Engineering from Paris XI University, Paris, France, in 1996. He is currently a Professor with the Electrical Engineering Department, Amirkabir University of Technology (Tehran Polytechnic), Tehran, Iran. He has authored 5 books and has authored or co-authored over 300 papers in refereed journals and local and international conferences. His research areas include wireless communication systems (RF technology and transceivers), RF/microwave/millimeter-wave/THz circuit and system design, electromagnetic (EM) modeling of active devices and circuits, high-frequency electronics (signal and noise), nonlinear modeling, and analysis of microwave devices and circuits.

Gholamreza Moradi was born in Shahriar, Iran in 1966. He received his B.Sc. in Electrical Communication Engineering from Tehran University, Tehran, Iran in 1989, and the M.Sc. in the same field from Iran University of Science and Technology in 1993. Then he received his Ph.D. degree in Electrical Engineering from Tehran Polytechnic University, Tehran, Iran in 2002. His research areas include applied and numerical Electromagnetics, Microwave measurement and antenna. He has published more than fifty journal papers and has authored/co-authored five books in his major. He is currently an Associate Professor with the Electrical Engineering Department, Amirkabir University of Technology (Tehran Polytechnic), Tehran, Iran. He is now a Visiting Professor at the University of Alberta.